

narrow bins. Using a phase-space background shape and constant-width Breit-Wigner curves to approximate the ρ^- , ρ^0 , and f^0 in a maximum-likelihood fit, we find the peaks of the ρ^0 and the ρ^- are, respectively, at 777 ± 5 and 744 ± 6 MeV and the widths are 135 ± 10 and 113 ± 16 MeV. Our mass resolution in the ρ region is about ± 12 MeV. Since the computed positions of the ρ peaks are quite sensitive to the background assumed, the apparent difference in position is less significant than the statistics alone would indicate.

IV. g^- MESON

The g meson in the dipion state has been observed in the charged as well as in the neutral state at different incident beam momenta.¹¹ Figure 1(c) shows a g^- peak centered at about 1600 MeV, having a width of about 200 MeV. The position seems slightly displaced from the value of about 1640 MeV, reported at the Vienna

¹¹ *Proceedings of the Fourteenth International Conference on High Energy Physics, Vienna, Austria, 1968*, edited by J. Prentki and J. Steinberger (CERN Scientific Information Service, Geneva, Switzerland, 1968), p. 119.

Conference,¹¹ but within our statistical accuracy the results are not in serious disagreement.

ACKNOWLEDGMENTS

This experiment was made possible by the help and cooperation of the Shutt bubble chamber group and the AGS personnel of Brookhaven National Laboratory. We are grateful to Dr. V. Hagopian for advice and useful discussions and to Dr. H. Brody and Dr. Y. L. Pan for their help in the experiment. We wish to thank A. Snyderman, W. Kononenko, R. Marshall, H. Casalunova, and the Pennsylvania Scanning and Measuring Staff for their assistance with the data analysis. The Notre Dame group would like to thank Dr. J. W. Andrews, Dr. I. Derado, and Dr. E. H. Synn for their contributions in the early phase of the work; they also acknowledge the assistance of J. B. Annable and the Notre Dame Scanning and Measuring Staff with the data analysis. One of us (H. Y.) would like to thank Professor A. C. Melissinos, Professor T. Yamanouchi, Professor T. Ferbel, and Professor R. L. Thews for useful discussions and encouragement.

Measurement of the Muon Polarization Vector in $K^+ \rightarrow \pi^0 + \mu^+ + \nu^\dagger$

D. CUTTS,* R. STIENING, AND C. WIEGAND

Lawrence Radiation Laboratory, University of California, Berkeley, California 94720

AND

M. DEUTSCH

Massachusetts Institute of Technology, Cambridge, Massachusetts 02139

(Received 9 April 1969)

We have studied the decay $K^+ \rightarrow \pi^0 + \mu^+ + \nu$ ($K_{\mu 3}$) in a spark-chamber experiment at the Bevatron. The data consist of 3133 events with μ - e decays and complete kinematics for $K_{\mu 3}^+$. We determined the muon polarization vector from the angular distribution of the decay electrons and related this measurement to a determination of the vector form-factor ratio, $\xi = f_-/f_+$. The data are statistically consistent with the assumption that ξ does not depend on momentum transfer. Assuming ξ constant, our result is $\xi = (-0.9 + 0.5/-0.4) + i(-0.3 \pm 0.5)$. If we analyze the data imposing the constraint that ξ be real, we find $\xi = -0.95 \pm 0.3$. The muon polarization along the direction predicted by these values for ξ is 0.9 ± 0.1 . In a calibration experiment, we find the muon longitudinal polarization in the decay $K^+ \rightarrow \mu^+ + \nu$ to be -1.0 ± 0.1 .

I. INTRODUCTION

THE current phenomenological theory of weak interactions successfully describes μ decay, a purely leptonic process, as well as neutron β decay and other strangeness-conserving semileptonic processes. We wish to test this description of weak interactions by studying strangeness-violating semileptonic processes.

The most readily available examples of such processes, experimentally, are the $K_{\mu 3}$ and $K_{e 3}$ decay modes of the K meson

$$K \rightarrow \pi + \mu + \nu \quad (K_{\mu 3})$$

and

$$K \rightarrow \pi + e + \nu \quad (K_{e 3}).$$

This work is a study of the $K_{\mu 3}$ decay.

The matrix element for $K_{\mu 3}$ decay is

$$\frac{G}{\sqrt{2}} \langle \pi^0 \mu^+ \nu | J_\lambda^\dagger J_\lambda^{h, \Delta s \neq 0} | K^+ \rangle,$$

† Work performed under the auspices of the U. S. Atomic Energy Commission.

* Present address: Department of Physics, State University of New York, Stony Brook, New York 11790.

where $G/\sqrt{2}$ is the weak-interaction coupling constant, $J_{\lambda}^{h,\Delta s \neq 0}$ is the strangeness-changing hadronic current, and J_{λ}^l is the leptonic current. Summation over the index λ is assumed ($\lambda=1, 2, 3, 4$). The specific form of J_{λ}^l is well known from β decay and muon decay; the form of $J_{\lambda}^{h,\Delta s \neq 0}$ is unknown. We can, however, describe it phenomenologically using the fact that the whole matrix element must be a scalar. Since J_{λ}^l has only vector and axial-vector terms, only the vector part of $J_{\lambda}^{h,\Delta s \neq 0}$ can contribute to the $K_{\mu 3}$ matrix element. (The axial-vector term of $J_{\lambda}^{h,\Delta s \neq 0}$ does not contribute as the K and π have the same intrinsic parity.) These assumptions restrict its form to

$$\langle \pi^0 | J_{\lambda}^{h,\Delta s \neq 0} | K^+ \rangle = f_+(q^2)(p_K + p_{\pi})_{\lambda} + f_-(q^2)(p_K - p_{\pi})_{\lambda}. \quad (1)$$

Here p_K and p_{π} are the K and π four-momenta. $f_+(q^2)$ and $f_-(q^2)$ are unknown parameters which may be complex and dependent on the four-momentum transfer between the K and the π ,

$$q^2 = (p_K - p_{\pi})^2.$$

In defining the parameters $f_+(q^2)$ and $f_-(q^2)$, we have written a general vector expression; there are two independent four-vectors in the K - π system, so there are two independent vector terms. The specific form of the expression is conventional.

We define the parameter $\xi(q^2)$ as the ratio of the two vector form factors:

$$\xi(q^2) \equiv f_-(q^2)/f_+(q^2).$$

In this study of the $K_{\mu 3}^+$ decay we measure directly the parameter $\xi(q^2)$. With this measurement we test the adequacy of the basic formalism to describe this strangeness-changing weak process. Additionally, we investigate the q^2 dependence of this parameter; the range of momentum transfer is large

$$M_{\mu}^2 < q^2 < (M_K - M_{\pi})^2$$

relative to that available in purely leptonic or other semileptonic decays, such as decay or neutron decay. The principle of time-reversal invariance can be tested by measuring the phase of ξ . Time-reversal invariance requires the form factors $f_+(q^2)$ and $f_-(q^2)$ to be relatively real, and consequently the phase of ξ to be 0° or 180° , for all values of q^2 . (Final-state interactions, which could introduce an imaginary part to ξ , have been shown to be negligible.¹) By comparing this measurement of ξ in $K_{\mu 3}^+$ decay with the measurements of ξ in $K_{\mu 3}^0$ decay, we can test the $\Delta I = \frac{1}{2}$ rule, which requires ξ to be identical for both modes. The principle of universality of the muon and the electron requires that the form factors be the same for $K_{\mu 3}$ and $K_{e 3}$ decays. Our determination of ξ is independent of μ - e universality. To test this principle, we can compare our measurement

¹ E. S. Ginsberg, Phys. Rev. **142**, 1035 (1966).

of ξ with the results for ξ of experiments which assume μ - e universality.

II. METHOD

We determine the parameter $\xi(q^2)$ by measuring the muon polarization for completely reconstructed $K_{\mu 3}$ events. As noted by MacDowell² and by Werle,³ the two-component theory of the neutrino requires that, for a specific kinematic configuration, the muon be completely polarized in some direction. In a theoretical paper, Cabibbo and Maksymowicz⁴ observed that the direction of the muon polarization vector for specified kinematics is a sensitive function of the parameter $\xi(q^2)$. They suggested the experiment to measure the muon polarization in completely reconstructed $K_{\mu 3}$ events, and thus directly measure ξ .

In our experiment, we determined the complete kinematics for $K_{\mu 3}$ decays from K^+ mesons at rest. For each decay, we defined a coordinate system relevant to that decay, a system to which we referred our measurement of the vector direction of the muon polarization. From the calculated kinematics, we constructed for each $K_{\mu 3}$ event three orthogonal axes, longitudinal, transverse, and perpendicular, given by

$$\begin{aligned} \hat{e}_L &= \mathbf{p}_{\mu} / |\mathbf{p}_{\mu}|, \\ \hat{e}_T &= \mathbf{p}_{\pi} \times \mathbf{p}_{\mu} / |\mathbf{p}_{\pi} \times \mathbf{p}_{\mu}|, \\ \hat{e}_1 &= \mathbf{p}_{\mu} / |\mathbf{p}_{\mu}| \times \mathbf{p}_{\pi} \times \mathbf{p}_{\mu} / |\mathbf{p}_{\pi} \times \mathbf{p}_{\mu}|. \end{aligned} \quad (2)$$

In this coordinate system, the muon polarization direction is given by⁴

$$\mathbf{P} = (A_L \hat{e}_L + A_T \hat{e}_T + A_1 \hat{e}_1) / |\mathbf{A}|, \quad (3)$$

where

$$\begin{aligned} A_L &= a_1(\xi) |\mathbf{p}_{\mu}| - \frac{a_2(\xi) |\mathbf{p}_{\mu}|}{m_{\mu}} \\ &\times \left[m_K - E_{\pi} + \frac{|\mathbf{p}_{\pi}|}{|\mathbf{p}_{\mu}|} (E_{\mu} - m_{\mu}) \cos \theta_{\pi\mu} \right] \\ &\quad - a_2(\xi) |\mathbf{p}_{\pi}| \cos \theta_{\pi\mu}, \\ A_T &= |\mathbf{p}_{\pi}| |\mathbf{p}_{\mu}| m_K \sin \theta_{\pi\mu} \operatorname{Im} \xi(q^2), \\ A_1 &= -a_2(\xi) |\mathbf{p}_{\pi}| \sin \theta_{\pi\mu}. \end{aligned}$$

Here

$$\begin{aligned} a_1(\xi) &= 2(m_K^2/m_{\mu}) [E_{\nu} + (E_{\pi}^{\max} - E_{\pi}) \operatorname{Re} b(q^2)], \\ a_2(\xi) &= m_K^2 + 2m_K E_{\mu} \operatorname{Re} b(q^2) + m_{\mu}^2 |b(q^2)|^2, \end{aligned}$$

and

$$\begin{aligned} b(q^2) &= \frac{1}{2} [\xi(q^2) - 1], \\ E_{\pi}^{\max} &= (m_K^2 + m_{\pi}^2 - m_{\mu}^2) / 2m_K. \end{aligned}$$

In these expressions, \mathbf{p}_{μ} and \mathbf{p}_{π} are the μ and π momenta; and E_{μ} , E_{π} , and E_{ν} are the energies of the μ , π , and ν in

² S. W. MacDowell, Nuovo Cimento **9**, 258 (1958).

³ J. Werle, Nucl. Phys. **6**, 1 (1958).

⁴ N. Cabibbo and A. Maksymowicz, Phys. Letters **9**, 352 (1964).

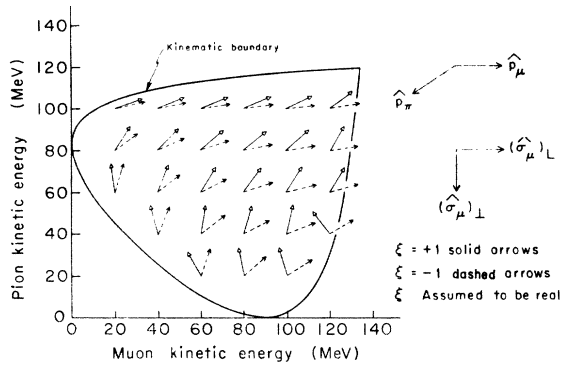


FIG. 1. Predicted direction of the muon polarization vector at various points in the $K_{\mu 3}^+$ Dalitz plot.

the K^+ rest system. m_K , m_π , and m_μ are the K^+ , π^0 , and μ^+ rest masses. For specified kinematics of the $K_{\mu 3}$ decay, the vector muon polarization direction, given by Eq. (3), is a function only of the parameter $\xi(q^2)$.

Figure 1 shows the muon polarization direction at various positions in the $K_{\mu 3}$ Dalitz plot, as predicted by Eq. (3). The solid and dashed arrows give the polarization directions at the kinematic point for $\xi = +1$ and $\xi = -1$, as measured in the coordinate system shown at the right. For this example, we assume ξ to be real, and independent of q^2 . Figure 1 illustrates the increased sensitivity to ξ of polarization measurements for events with low π^0 energy, where the polarization is largely perpendicular. As defined previously,

$$q^2 = m_K^2 + m_\pi^2 - 2m_K E_\pi,$$

so that high π^0 energy corresponds to low q^2 ; in this

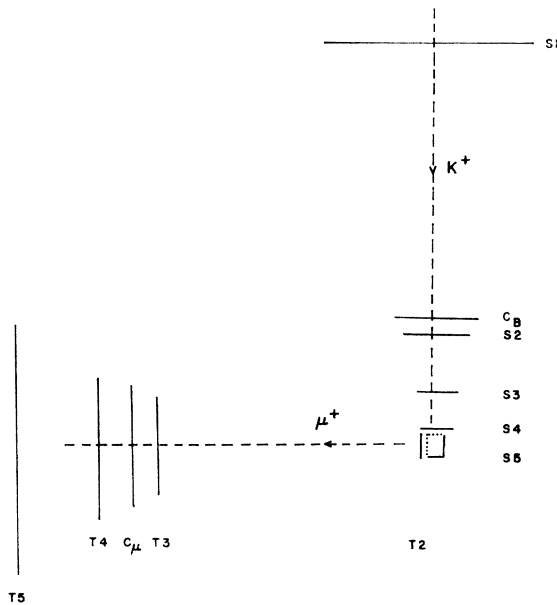


FIG. 2. Diagram of scintillation counters used in the experiment.

region of the Dalitz plot, the muon polarization is almost purely longitudinal, and relatively independent of ξ .

In this experiment, we measured the muon polarization vector by stopping μ^+ 's from $K_{\mu 3}$ decays, and observing the direction of the electron in the subsequent decays

$$\mu^+ \rightarrow e^+ + \nu_e + \bar{\nu}_\mu.$$

From the experimentally verified decay spectrum^{5,6} for a muon with polarization \mathbf{P} , we have

$$dw/d(\cos\theta) \propto \frac{1}{2}(1 + \frac{1}{3}|\mathbf{P}| \cos\theta), \quad (4)$$

where

$$\cos\theta = (\mathbf{P}/|\mathbf{P}|) \cdot \hat{p}_e.$$

Equation (4) gives the μ -decay probability in terms of the direction \hat{p}_e of the decay electron, and shows that the electron-vector direction preferentially lies along the direction of the muon polarization. In our experiment, we inferred the muon polarization direction from the observed angular distribution of the decay electrons. As will be described later, we verified the analyzing power of our apparatus by direct experimental measurements.

III. EXPERIMENTAL APPARATUS

A. Scintillation Counters and Spark Chambers

K^+ mesons were degraded to rest in a scintillation-counter telescope at the second focus of a 500-MeV/ c separated K^+ beam at the Bevatron. A water Čerenkov counter C_B preceded carbon blocks interspaced between counters S2, S3, S4, S5, forming a compact telescope as illustrated in Fig. 2. The hollow cup-shaped counter S5, surrounding the K^+ stopping region, was 3 in. in length along the beam direction and 2×2.5 in. in cross section; the interior was filled with carbon dust of density 0.85 g/cm³. This counter enclosed all sides of the stopping region except the side through which K^+ mesons entered, and the side toward the decay-particle range chamber. These two sides were covered by counters S4, in the beam telescope, and by T2, the first of 5 counters in the decay-particle telescope. Figure 2 is a horizontal cross section of the apparatus, showing all the counters used in the experiment as seen from above. The counter S1 covered the exit aperture of the last magnet element of the beam-transport system, a quadrupole doublet; the distance from S1 to the stopping region inside S5 was 3 ft.

In order to consider a beam particle as being a stopping K^+ , we required the coincidence of pulses from the scintillation counters in the beam telescope

$$K_{\text{stop}} = S1 \cdot S2 \cdot S3 \cdot S4 \cdot \bar{C}_B \cdot \bar{S}5.$$

The counter S5 surrounding the stopping region was in prompt anticoincidence, and vetoed the event upon

⁵ C. Bouchiat and L. Michel, Phys. Rev. **106**, 170 (1957).

⁶ T. D. Lee and C. S. Wu, Ann. Rev. Nucl. Sci. **15**, 381 (1965).

detecting a particle within 6 nsec of the time a particle entered the beam telescope. The 2-in.-thick water Čerenkov counter C_B , also in anticoincidence, rejected fast particles (primarily π^+) in the beam, as did the requirement that the pulses from the beam counters be greater than those from minimum-ionizing particles.

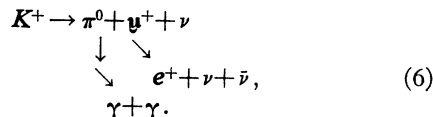
The counters forming the decay-particle telescope are shown in Fig. 3, a vertical cross section of the apparatus. In this figure, the K^+ beam is directed out of the page. With the counter T5 in anticoincidence, the telescope T2-T3-T4 selected particles leaving the K^+ stopping region which came to rest in the chamber between T4 and T5. The water Čerenkov counter C_μ was used as a veto against fast-decay particles, including μ^+ from the decay $K^+ \rightarrow \mu^+ + \nu$ and electrons from the decay $K^+ \rightarrow \pi^0 + e^+ + \nu$; most of these particles were also excluded by the range requirement imposed by T5.

To be considered an acceptable K^+ event, the decay-particle signal had to come 6 to 44 nsec following the signal of a stopping K^+ . The minimum allowed time between a K stop and the K decay was chosen to insure a rejection of better than 250/1 against K^+ decays in flight and other prompt events. The logic corresponding to an acceptable K^+ decay was

$$\begin{aligned} K_{\text{decay}} &= (K_{\text{stop}}) \cdot (\text{good decay})_{\text{delayed}} \\ &= (S1 \cdot S2 \cdot S3 \cdot S4 \cdot \bar{C}_B \cdot \bar{S5}) \\ &\quad \cdot (T2 \cdot T3 \cdot T4 \cdot \bar{C}_\mu \cdot \bar{T5})_{\text{delayed}}. \end{aligned} \quad (5)$$

This coincidence represented the criterion for an electronic trigger.

The events selected by the scintillation counters were recorded on film by photographing tracks left in spark chambers arranged as shown in Fig. 3. In order to determine completely the kinematics for each $K_{\mu 3}$ decay, we observed the track of a stopping μ^+ and the tracks of electron showers from conversion of γ rays. The π^0 produced in the $K_{\mu 3}$ decay itself decayed with a mean life of 10^{-16} sec to two γ rays



To measure the muon polarization, we observed the track of the electron from the subsequent μ - e decay. The five particles we detected with spark chambers are boldfaced in Eq. (6). Two aluminum-plate chambers, each with two gaps, were embedded in the beam telescope between counters S3 and S4. These chambers indicated the track of the K^+ before stopping, aiding in the reconstruction of the K^+ decay position within the carbon stopper. To observe the γ -ray showers we used three 36-gap chambers surrounding the stopping region as shown in Fig. 3, a vertical cross section. The plates of these chambers consisted of sheets of lead each 0.8 mm thick and sandwiched between two 0.3-mm aluminum sheets. To ensure rejection of charged

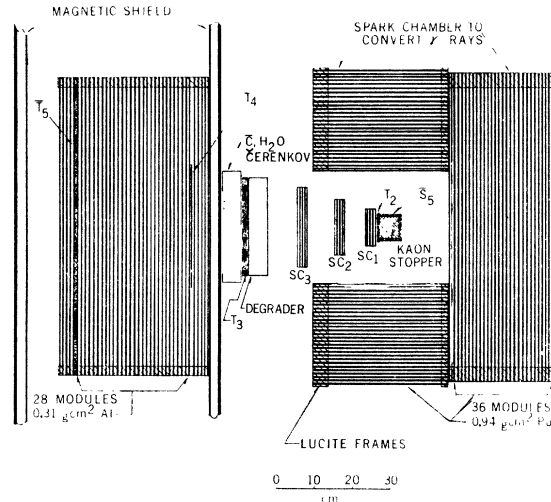


FIG. 3. Vertical cross section of the apparatus.

particles entering the shower chambers, the two plates in each chamber closest to the K^+ stopping region were thin aluminum sheets, and were used in anticoincidence.

We used three 4-gap spark chambers, labeled SC1, SC2, SC3 in Fig. 3, to measure the direction of the charged particle from the K^+ decay. These thin-plate aluminum chambers were placed directly after the counter T2 in the decay-particle telescope, before the degrader, to reduce the effect of scattering in distorting the measurement of the initial decay direction.

The coincidence criteria for an acceptable event required the μ^+ from a $K_{\mu 3}$ decay to stop between counters T4 and T5. As shown in Fig. 3, these counters were embedded in a 36-gap aluminum-plate spark chamber. Between counters T4 and T5 was a 28-gap spark-chamber module whose total thickness was 9.9 g/cm² of aluminum, while ahead of counter T4 and beyond counter T5 were 4-gap modules, constructed of $\frac{1}{32}$ in. and $\frac{1}{16}$ in. plates, respectively. With this 36-gap spark chamber, we measured the range of the muon from $K_{\mu 3}$ decay and the direction of the electron momentum in the subsequent μ - e decay. We enclosed the entire chamber in a magnetic shield to reduce precession of the muon and consequent depolarization.

B. Experimental Technique

The requirement that the charged particle from the K^+ -decay stop between counters T4 and T5 imposed a restriction on its range. We placed a degrader in the decay-particle counter telescope ahead of counter T3 to define this range acceptance. We changed this degrader to study K^+ -decay particles with different range. Table I lists the degrader used to obtain data for various K^+ decay modes.

We studied $K_{\mu 3}$ decays under two degrader conditions; 83% of our $K_{\mu 3}$ events were obtained with degrader *a*, 1 in. of aluminum. With this degrader, the

TABLE I. Degradar conditions.

Events	Degradar	Decay particle	KE spectrum accepted (direct path)
$K_{\mu 3}$ (degrader <i>a</i>)	1 in. Al	μ^+	61–81 MeV
$K_{\mu 3}$ (degrader <i>b</i>)	$\frac{3}{8}$ in. Al	μ^+	52–73 MeV
$K_{\pi 2}$	$2\frac{1}{4}$ in. Al	π^+	108.6 MeV
$K_{\mu 2}$	1 in. Al + $2\frac{1}{8}$ in. Cu	μ^+	151.7 MeV

range criterion for a direct path from the K^+ -decay position selected μ^+ with kinetic energy between 61 and 81 MeV. We chose this window in the μ^+ spectrum to exclude from the $K_{\mu 3}$ data much of the background from both $K_{\pi 2}$ decays ($K^+ \rightarrow \pi^+ + \pi^0$), for which $T_{\pi^+} = 108.6$ MeV, and τ' decays ($K^+ \rightarrow \pi^+ + \pi^0 + \pi^0$), where the end point of the π^+ spectrum is 53.2 MeV. Additional $K_{\mu 3}$ data were taken with a $\frac{3}{8}$ -in. aluminum degrader. To aid in our analysis of the $K_{\mu 3}$ data, we studied events with the μ^+ from $K_{\mu 2}$ decays ($K^+ \rightarrow \mu^+ + \nu$), and the π^+ from $K_{\pi 2}$ decays ($K^+ \rightarrow \pi^+ + \pi^0$). The different amounts of degrader placed in the decay-particle telescope for these studies are given in Table I.

We triggered the spark chambers upon the electronic signal of an acceptable K^+ decay as defined by Eq. (5). For each event, we recorded photographically the tracks in 9 spark chambers: 2 beam chambers, 3 shower chambers, 3 decay-particle tracking chambers, and the range chamber. With the exception of the range chamber, all the spark chambers were fired promptly with the coincidence signal; the total delay from the time of a K^+ stop to the presence of voltage on the spark-chamber plates was 340 nsec. We delayed the trigger signal to the muon range chamber for 3.5 μ sec. The μ^+ , stopped between counters T4 and T5, decayed with a mean life of 2.2 μ sec; with our delay in triggering this chamber, we observed the electron track in 80% of the μ - e decays. In order to maintain both the muon track and the track of the decay electron for as long as 3.5 μ sec, we limited the dc clearing field on the range spark chamber to 6.9 V per cm. On the 8 chambers triggered promptly, we applied between 47 and 63 V per cm to clear residual tracks. In a background study, we obtained some data of $K_{\mu 3}$ events for which the range chamber was fired promptly; for these events the trigger delay time on all the chambers was 340 nsec and the clearing voltage was 40 V. All the spark chambers were filled with neon, purified through a closed-circuit recirculation system.

In addition to spark-chamber tracks of particles, we recorded on film with each event, fiducial lamps mounted on the apparatus and bright grid lines defining the position of the data. We were careful to put many reference points on the film in order to simplify its subsequent automatic computer scanning. For each photograph, we lit numeral lamps giving the event number; this number was displayed as well by a row of binary-coded lights, to be computer-scanned. A second

row of binary-coded lights gave digitized information about the event: whether or not a particle was detected by counter S1 in the beam telescope within 20 nsec of the K^+ decay, and whether or not the counter S5 detected a particle within the full-time interval allowed for a K^+ -decay trigger. We digitized also for each event the time between the K -stop signal and the signal of the K decay, and displayed this information with binary-coded lights. The flashed lamps and all 18 views of the spark chambers were recorded on a 24×36 mm frame of Tri-X film, using a lens opening of $f/8$.

IV. ANALYSIS PROCEDURE

A. Selection of Events

We scanned a total of 80 000 pictures for $K_{\mu 3}^+$ events with SPASS, the automatic computer-scanning system developed by Rudloe *et al.* at MIT.⁷ With this system, we measured the position of tracks in all spark chambers except the muon range chamber. In the scan of the γ -ray chambers, we measured the spark count associated with each shower in addition to its conversion point. For each event we obtained, as well, the digitized information from the lamps. Using information from the SPASS scanning we selected 10 000 events to be hand scanned for μ - e decays on the SCAMP machine at Lawrence Radiation Laboratory (LRL). On SCAMP we measured the direction of the incoming μ^+ track in the range chamber, the position of the μ^+ stop, and the vector direction of the decay electron. We selected for reconstruction as $K_{\mu 3}$ events a further restricted sample, using information from both the SPASS and the SCAMP scanings. The criteria imposed based on the SPASS measurements were:

- (1) Two γ -ray showers were unambiguously stereo reconstructed, with conversion points not in the first two gaps of the chamber.
- (2) No pulse in coincidence with the muon was observed in the cup-shaped counter S5 which surrounded the K^+ stopping position, shielding the decay point from the shower chambers.
- (3) The reconstructed position of the K^+ stop must have been in the carbon stopper within the box of counters.
- (4) Neither of the two showers measured was at an edge of the chambers.
- (5) The opening angle of the two γ rays was greater than 65°.
- (6) The event did not satisfy $K_{\pi 2}$ kinematics. From the initial charged-particle direction and the directions of each γ ray relative to the K -stop position, we calculated the γ -ray directions in the π^0 c.m. system, assuming the event to be a $K_{\pi 2}$ decay, and the quantity δ :

$$\delta = \hat{k}_1' \cdot \hat{k}_2'$$

⁷H. Rudloe, M. Deutsch, and T. Marill, Commun. Assoc. Comput. Machin. **6**, 332 (1963).

Here, \hat{k}_1' and \hat{k}_2' are the γ -ray directions as transformed to the postulated π^0 rest system. K_{π^2} kinematics requires that $\delta = -1$; our criterion for acceptance of the event was that $\delta > -0.9$.

(7) The line of flight of the charged decay particle as measured in the thin chambers SC1, SC2, SC3 did not have a kink. We required that $\hat{p}_1 \cdot \hat{p}_2 > 0.998$, where \hat{p}_1 and \hat{p}_2 are the particle directions calculated from tracks in SC1 and SC2, and in SC2 and SC3.

(8) The distance of closest approach of the calculated K^+ line of flight to the decay particle line of flight was less than 1.0 cm. We took as the K^+ stopping position the point on the muon line of flight closest to the incident K^+ line of flight.

We used the hand scanning on SCAMP to select events with the following characteristics:

(1) The scanner observed in the range-chamber tracks of a muon entering and stopping and of an electron from the subsequent μ - e decay. Events without such tracks were rejected. In about 2% of the data (otherwise acceptable as K_{μ^3} events), the scanner was uncertain whether or not the tracks corresponded to those of a muon and its decay electron. After a rescan by a physicist, we considered most of these events (51 pictures) to have acceptable range-chamber tracks. Events with both tracks extending from the μ - e vertex to the front of the range chamber were measured twice, assuming one track and then the other to be the μ^+ ; we selected that assignment which best matched the line of flight measurement on SPASS from the chambers SC1, SC2, SC3. For each event, we calculated the distance at the degrader between the μ^+ line of flight measured from SC1, SC2, SC3 and the line of flight seen in the range chamber. If this distance was greater than 6 cm, the event was remeasured by a physicist; 1% of the total data (otherwise acceptable as K_{μ^3} events) were in this category, of which 4 events (0.1%) were rejected by the rescan.

(2) The scanner agreed with SPASS that there were exactly two γ -ray showers, and that neither γ ray converted in the first two gaps of its chamber.

(3) The electron decay direction was not within a forward cone about the initial muon direction. To eliminate events with μ - e decays in a region of low scanning efficiency, we rejected all events unless $\hat{p}_e \cdot \hat{p}_\mu < 0.9$.

(4) The μ - e vertex position was not in the counter T4. This cut eliminates events with the muon depolarized by stopping in the plastic scintillator.

After the selection based on both the SPASS and the SCAMP measurements, the remaining 3549 events were analyzed as candidates for K_{μ^3} decays. The procedures in reconstructing the data in terms of K_{μ^3} kinematics are described in Sec. IV B. Following this analysis our

final data sample consisted of 3133 completely reconstructed K_{μ^3} events with observed μ - e decays.

B. Reconstruction of K_{μ^3} Kinematics

For each event we had the following data: (1) Range of the charged particle originating from the K^+ decay. (2) Direction of motion of the charged particle originating from the K^+ decay. (3) Position of the K^+ decay. (4) Positions of the points where two γ rays produce showers by conversion. (5) The number of sparks associated with each γ -ray shower. We calculated the energy of the charged particle, assuming it to be a muon, from its stopping position in the range chamber. We based this calculation on comparisons of measured range with the predicted range of particles with known energy: π^+ from K_{π^2} and μ^+ from the K_{μ^2} -decay mode. We took the K^+ -decay position as that point along the line of flight of the track in SC1, SC2, and SC3 closest to the K^+ line of flight as measured by two spark chambers in the beam. From the K^+ -decay position and the γ -ray conversion points, we determined the unit vectors $\hat{\epsilon}_{\gamma 1}$, $\hat{\epsilon}_{\gamma 2}$ pointing in the direction of each γ ray.

With the measured quantities E_μ , \mathbf{p}_μ , $\hat{\epsilon}_{\gamma 1}$, $\hat{\epsilon}_{\gamma 2}$, the kinematics of the decay was not uniquely determined. In general, there were two solutions compatible with the data, corresponding to different momenta of the π^0 . The ambiguity was removed by determining the γ -ray energies from their measured spark count, using a relation derived from a study of showers of known energy in K_{π^2} data. For K_{π^2} events, we knew the π^0 energy and direction of motion; we could calculate each γ -ray energy from the position in the apparatus where a shower was produced by conversion, and compare this energy with the observed number of sparks. Using the relation between energy and spark count, we determined the γ -ray energies for each of the K_{μ^3} events, and thereby arrived at a complete solution of K_{μ^3} kinematics.

In order to analyze the muon polarization, it was necessary to define for each event a coordinate system with axes corresponding to the orientation of the K -decay configuration, rather than to directions in the lab. Knowing the muon and pion momenta \mathbf{p}_μ and \mathbf{p}_π , we constructed three orthogonal axes: a longitudinal axis along the muon momentum, a transverse axis out of the decay plane (in the sense $\mathbf{p}_\pi \times \mathbf{p}_\mu$), and a perpendicular axis in the decay plane towards the pion momentum. From the measurement of the laboratory direction of the electron in the μ - e decay, we calculated the electron direction relative to this K -decay coordinate system [Eq. (2)]. The solution of the K_{μ^3} kinematics and the calculation of the electron decay direction in this coordinate system completed the reconstruction of the event.

TABLE II. Calculation of uncertainty limits in a likelihood analysis.

Number of likelihood parameters	Value of L/L^{\max} at limit of:	
	1 standard deviation	2 standard deviations
1	$e^{-0.5}$	e^{-2}
2	$e^{-1.14}$	$e^{-3.10}$

C. Muon Polarization Analysis

We determined the parameter ξ directly from the observed electron angular distributions in the μ - e decays. We assumed that the muon in each $K_{\mu 3}$ event was fully polarized in a direction given by Eq. (3). As in Eq. (4), we defined a normalized probability distribution for the electron direction in μ - e decays, given the predicted direction of the muon polarization, $\hat{\sigma}_\mu$. This direction, for each event, is a function of the specific kinematics as well as the value of the parameter ξ . We took the magnitude of the polarization along this direction to be 1. We constructed the likelihood function, depending only on ξ , as the product over all the events of the separate probability distributions

$$L(\xi) = \prod_{i=1}^N \frac{1}{c_i(\xi)} \{1 + \frac{1}{3} [\hat{p}_e \cdot \hat{\sigma}_\mu(\xi)]_i\}. \quad (7)$$

The muon polarization direction is given by Eq. (3) as a vector in the coordinate system $(\hat{\epsilon}_L, \hat{\epsilon}_T, \hat{\epsilon}_1)$ defined by the K decay; \hat{p}_e is the observed direction of the decay electron in this system, and $\hat{\sigma}_\mu$ is a unit vector along the predicted direction of polarization, \mathbf{P} . Both the electron and the polarization directions are specific to each event as reconstructed. The normalization factor $c(\xi)$ for the i th event has the form

$$c_i(\xi) = (1 + \cos\theta_0) \{1 - \frac{1}{6} (1 - \cos\theta_0) [\hat{p}_e \cdot \hat{\sigma}_\mu(\xi)]_i\}.$$

The factor corrects the likelihood for the elimination of μ - e decays within a forward cone about \hat{p}_μ of half-angle $\theta_0 = \cos^{-1}(0.9)$. Our result for ξ is that value which maximizes the likelihood function, Eq. (7). We found the uncertainty in this determination by noting the values of ξ for which the likelihood function was reduced from its maximum by a specified factor. We made the likelihood analysis for various assumptions about ξ : ξ real and constant, ξ complex and constant, or ξ real but energy-dependent. Consequently, the likelihood $L(\xi)$ was a function of 1 or 2 parameters. Table II gives the value of the likelihood, with respect to its maximum, used to determine the uncertainty in the measurement of ξ . It should be emphasized that the appropriate limits of uncertainty for a two-parameter likelihood are markedly greater than those appropriate for a one-parameter likelihood.⁸

⁸ D. J. Hudson, CERN Report No. 64-18, 1964 (unpublished); J. Orear, University of California Lawrence Radiation Laboratory Report No. UCRL-8417, 1958 (unpublished).

Having determined the parameter ξ from the polarization data, we reanalyzed the $K_{\mu 3}$ events to measure the magnitude of the muon polarization along the predicted direction σ_μ . We constructed a one-parameter likelihood function similar to that used to find ξ [Eq. (7)]. This likelihood is

$$L(P) = \prod_{i=1}^N \frac{1}{c_i(\xi, P)} \{1 + \frac{1}{3} P [\hat{p}_e \cdot \hat{\sigma}_\mu(\xi)]_i\} \quad (8)$$

with

$$c_i(\xi, P) = (1 + \cos\theta_0) \{1 - \frac{1}{6} P (1 - \cos\theta_0) [\hat{p}_e \cdot \hat{\sigma}_\mu(\xi)]_i\}.$$

The likelihood is a function of the magnitude P of the muon polarization; given ξ , we maximized the likelihood to determine P . The uncertainty in the measurement of P was found by calculating values of $L(P)/L^{\max}$ as in Table II.

V. KNOWN SOURCES OF ERROR

A. Uncertainties in Analysis of $K_{\mu 3}$ Events

Each event of our final $K_{\mu 3}$ data sample provides a separate measurement of $\xi(q^2)$. For each event with specified kinematics, we determine the parameter $\xi(q^2)$ by correlating the vector direction of the electron momentum in μ - e decay with the predicted muon polarization direction. The likelihood analysis gives as our result for ξ that value most compatible with the individual measurements of ξ from each event. With this method of determining ξ , it is not necessary to know the dependence of the detection efficiency upon the position of the event in the $K_{\mu 3}$ Dalitz plot. Since the measurement of ξ is made for each event, the result for all the data is independent of their Dalitz-plot distribution. It is important, however, that the positions in the Dalitz plot of the detected events be correctly determined.

Using a Monte Carlo analysis, we studied the effect of the measurement uncertainties on reconstruction of $K_{\mu 3}$ events. We generated by computer a large artificial sample of $K_{\mu 3}$ events with μ - e decays as predicted for a given value of the parameter ξ , and selected those events which would have been detected by the apparatus. For each artificial event we changed randomly the kinematical quantities by small amounts to simulate the effect of the measurement errors on the actual $K_{\mu 3}$ events. We reconstructed and analyzed these Monte Carlo events in a manner identical to that used for the $K_{\mu 3}$ data. We found that the result for ξ was insensitive to the presence of our known measurement uncertainties. In particular, both the 30-50% uncertainty in the γ -ray energy measurements and the ± 3 -MeV error in the μ^+ energy had little effect on the kinematic reconstruction, and negligible effect on the determination of ξ .

The reconstruction of the π^0 vector momentum was the crucial step in establishing the kinematics of each

$K_{\mu 3}$ event. We used the γ -ray energies, estimated from the shower spark counts, to choose between two predicted values of the π^0 momentum. As discussed above, we found by Monte Carlo studies that the presence of our measurement uncertainties in the γ -ray energies had no significant effect on the determination of ξ . Additionally, we studied the actual $K_{\mu 3}$ data to see whether or not events with incorrectly chosen π^0 momentum were present in an amount which significantly biased our result for ξ . Faulty π^0 reconstruction leads to two systematic effects, dependent on the direction of motion and on the energy of the π^0 . If the wrong π^0 solution is chosen, a faulty K -decay coordinate system [Eq. (2)] will be constructed. The incorrect π^0 energy will lead to a further error in the prediction of the muon polarization direction as a function of ξ . We separated the actual $K_{\mu 3}$ data into batches with the two possible π^0 vector directions close to each other, or not close, and with the two possible π^0 energies, nearly identical or different. We determined, from each of these samples, values for ξ statistically consistent with each other and with the result for ξ from all the data. There was no evidence for the presence of a systematic error due to incorrect solutions of the π^0 reconstruction.

Because of the limited geometrical acceptance of the shower chambers, we detected only one of the γ rays for many $K_{\mu 3}$ decays. The presence of background tracks in the shower chambers could then allow faulty reconstructions of these $K_{\mu 3}$ events. We estimated the frequency and distribution of background tracks from pictures taken of $K_{\mu 2}$ decays. There were no γ rays associated with $K_{\mu 2}$ decays, but for 5% of the events, a random track was interpreted as being a γ -ray conversion shower. In a Monte Carlo analysis, we added data to $K_{\mu 3}$ decays to simulate the presence of these background tracks. We found the number of incorrectly reconstructed $K_{\mu 3}$ events to be negligible.

We studied the effect on the result for ξ of variations in the criteria used to select $K_{\mu 3}$ events. Since the muon polarization vector and ξ were related for each kinematical configuration, each event provided a separate determination of ξ . For this reason, the use of arbitrarily rigid kinematical selection criteria did not bias the measurement of ξ . We analyzed our $K_{\mu 3}$ data repeatedly, using various selection criteria. We found the determination of ξ insensitive to changes in the selection criteria.

We determined ξ by correlating the kinematics of each $K_{\mu 3}$ event with the direction of the muon polarization vector as found from the μ - e decay. We calibrated the polarization measurement by studying the angular distribution of the electron momentum vector for $K_{\mu 2}$ events, with μ - e decays in the range chamber. For these events, we defined three orthogonal axes: a longitudinal axis $\hat{\epsilon}_L$ along the direction of the muon, and axes $\hat{\epsilon}_a$, $\hat{\epsilon}_b$ related to fixed directions in the laboratory. In Fig. 4, we show the distribution of the observed electron direction with respect to the coordinate system ($\hat{\epsilon}_L, \hat{\epsilon}_a, \hat{\epsilon}_b$);

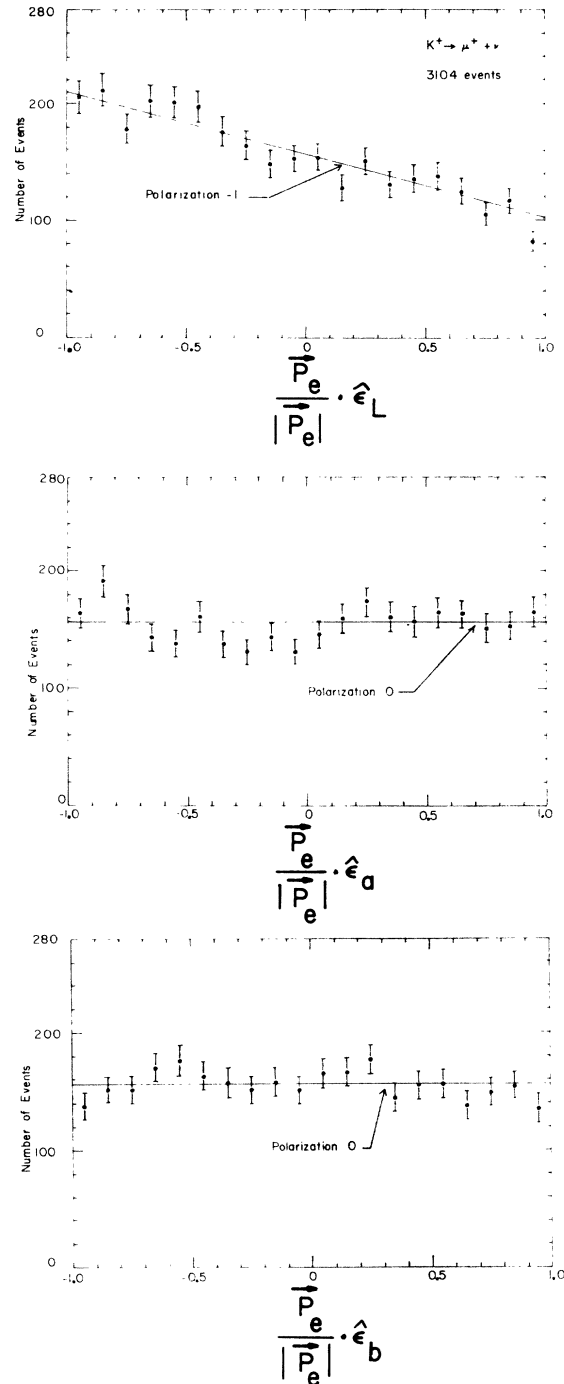
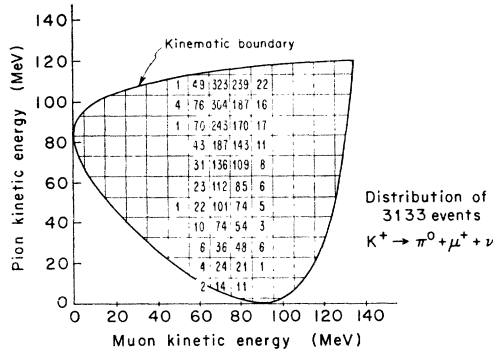


FIG. 4. Angular distribution of the electron momentum vector in μ - e decays, from 3104 $K_{\mu 2}^+$ events, referred to the axes $\hat{\epsilon}_L$, $\hat{\epsilon}_a$, $\hat{\epsilon}_b$.

the results of the likelihood analysis for the muon polarization components are

$$P_L = -1.0 \pm 0.1, \quad P_a = 0.0 \pm 0.1, \quad P_b = -0.1 \pm 0.1.$$

The measurement of the muon longitudinal-polarization component is in agreement with the expected value of

FIG. 5. Dalitz plot of 3133 $K_{\mu 3}^+$ events.

-1 for $K_{\mu 2}$ decays. This result is consistent with the assumption that there was no effective depolarization of the muon by the apparatus or the analysis techniques. The measurement of the muon polarization components along axes $\hat{\epsilon}_a$, $\hat{\epsilon}_b$ investigates possible dependence of the detection efficiency upon the orientation of the μ - e decay plane in the apparatus; the results for these components is consistent with the absence of such dependence.

A potential source of systematic error in the polarization measurement was our inability to observe μ - e decays in cases where the e^+ track was in the same direction as the track of the μ^+ before stopping. To correct for this effect, we eliminated all events having μ - e decays within a forward cone about the muon direction; we incorporated this selection into the polarization analysis by modifying the likelihood normalization. We chose the angle of the forward cone to more than cover decay directions for which the scanning efficiency was poor. As with our other selection criteria, the result for ξ is insensitive to variations in this cutoff. Except for this loss of forward decays, our detection of μ - e decays was essentially independent of the e^+ direction and energy.

Among sources of depolarization was the presence of a magnetic field in the range chamber, causing the μ^+ polarization vector to precess in the interval before the μ - e decay. To reduce this effect, we enclosed the range chamber in an iron shield; the measured field of less than 200 mG in the decay region produced insignificant depolarization. Measurement errors in the direction of the individual e^+ track had little effect on the determination of the polarization direction, as the e^+ decay directions are broadly distributed about the μ^+ polarization vector. We calculated that our $\pm 10^\circ$ uncertainty in the e^+ decay angles introduced an effective depolarization of less than 1%. We found by Monte Carlo studies that the determination of ξ is unaffected by muon depolarizations as large as 10%. Since ξ is found from the direction of the muon polarization vector, the primary effect of depolarization is to increase the uncertainty in the result for ξ .

B. Presence of Background Events in $K_{\mu 3}$ Data

We considered events other than $K_{\mu 3}$ decays which could be present as background in the data. Such events must pass the selection criteria described previously. They must have two apparent showers in the γ -ray chambers, and a track in the range chamber with an apparent μ - e vertex. They must be kinematically reconstructable as $K_{\mu 3}$ events, but fail the kinematic test for a $K_{\mu 2}$ decay. Using Monte Carlo techniques, we generated large samples of artificial events, and studied the acceptance of the apparatus and selection criteria for background events relative to the acceptance for $K_{\mu 3}$ events. In addition to these calculations, we determined experimentally the actual contamination of our data by events whose frequency of apparent μ - e decays did not follow the μ^+ lifetime. We obtained a sample of $K_{\mu 3}$ events with a "prompt" (340-nsec) trigger on the range chamber, instead of the usual 3.5- μ sec delayed trigger. Knowing the delay times, we calculated the relative fractions of μ - e decays expected for each sample; from the number of apparent μ - e decays observed we determined the contamination of the data by events without μ - e decays.

The backgrounds considered are those due to the following K^+ decay modes:

$$\begin{aligned} K^+ &\rightarrow \pi^+ + \pi^0, & (K_{\pi 2}) \\ K^+ &\rightarrow \pi^+ + \pi^0 + \pi^0, & (\tau') \\ K^+ &\rightarrow \pi^+ + \pi^0 + \gamma, & (K_{\pi\pi\gamma}) \\ K^+ &\rightarrow \pi^0 + e^+ + \nu, & (K_{e3}). \end{aligned}$$

The $K_{\pi 2}$ decay was the most serious source of background events in the $K_{\mu 3}$ data. For the $K_{\pi 2}$ mode, we estimated the contributions of two sources of background: $K_{\pi 2}$ decays with a π^+ nuclear interaction in the range chamber, and $K_{\pi 2}$ decays with a π^+ decay in flight ($\pi^+ \rightarrow \mu^+ + \nu$). To determine the fraction of $K_{\pi 2}$ events which pass the $K_{\mu 3}$ selection criteria, we studied $K_{\pi 2}$ data obtained with additional degrader placed ahead of the range chamber. In Table III, we list the results of the background calculations. Two sources, K_{e3} decays and $K_{\pi 2}$ decays with a π^+ interaction in the range chamber, have " μ - e decays" whose frequency is independent of the time delay on the range-chamber

TABLE III. Results of background calculations.

Source of background	Est. fraction background/ $K_{\mu 3}$ events	Does frequency of "decays" follow μ^+ lifetime?
$K^+ \rightarrow \pi^+ + \pi^0 (K_{\pi 2})$		
with π^+ decay in flight	2.9×10^{-2}	yes
with π^+ nuclear interaction	$< 5.3 \times 10^{-2}$	no
$K^+ \rightarrow \pi^+ + \pi^0 + \pi^0 (\tau')$	5.0×10^{-4}	yes
$K^+ \rightarrow \pi^+ + \pi^0 + \gamma (K_{\pi\pi\gamma})$	1.4×10^{-2}	yes
$K^+ \rightarrow \pi^0 + e^+ + \nu (K_{e3})$	0.8×10^{-2}	no

trigger. The analysis of the prompt data shows that the total contribution of all such backgrounds was $(3 \pm 2)\%$ of the $K_{\mu 3}$ data. The estimated contribution of other possible backgrounds is less than 5%.

We have studied the effect of these backgrounds on our determination of ξ by adding these events to $K_{\mu 3}$ events generated in a Monte Carlo analysis. From this simulated data, our analysis determined a value of ξ statistically unchanged from the value used to generate the $K_{\mu 3}$ events. The primary effect of the presence of these backgrounds was to enlarge slightly the error limits assigned to ξ by the likelihood analysis.

VI. RESULTS

A. Study of $K_{\mu 3}^+$ Decay

We obtained 3133 completely reconstructed $K_{\mu 3}$ events with observed μ - e decays. The Dalitz plot of these events is shown in Fig. 5, where for clarity we have grouped the events in bins of 20 and 10 MeV in π^0 and μ^+ kinetic energy, respectively. Figure 6 gives the angular distributions of the electron momentum vector for the μ - e decays associated with the 3133 $K_{\mu 3}$ events which satisfy all the selection criteria. These distributions refer to the coordinate system $\hat{\epsilon}_L, \hat{\epsilon}_T, \hat{\epsilon}_1$ [Eq. (2)] defined for each event. For illustration, the data are grouped in bins of 0.1 in the cosines. The lines drawn show the distributions expected for decays of muons with average polarization components as given by a likelihood analysis of the data.

As seen in Fig. 1, muons from events with high π^0 energy are expected to be strongly polarized in the longitudinal direction. This prediction agrees with the data shown in Fig. 6, an average over the Dalitz plot, and hence heavily weighted toward high T_{π^0} . The component of polarization out of the decay plane is -0.1 ± 0.1 , which is consistent with zero and hence with time-reversal invariance; while the perpendicular component is small and negative, as predicted in Fig. 1. Since these components are averages over the Dalitz plot, they are not expected to form a unit vector; it is for a particular event, with specified kinematics, that the muon should be fully polarized in some direction. In Table IV, we tabulate the results for the μ^+ polarization components for all the events and in separate bins in the π^0 kinetic energy. For each bin, we list the

TABLE IV. Muon polarization components, $K_{\mu 3}^+$ events.

T_{π^0} (MeV)	$\langle q_{\mu}^2 \rangle$ (MeV ²)	Events	P_L	P_T	P_1	ΔP
>76.5	3.70×10^4	2258	+0.9	-0.1	-0.2	each ± 0.1
46.5-67.5	7.18×10^4	488	+0.8	-0.2	-0.1	each ± 0.2
28.5-46.5	9.09×10^4	265	+0.8	-0.2	-0.8	each ± 0.3
0.0-28.5	11.0×10^4	122	-0.1	+0.5	-1.1	each ± 0.5
all events	4.95×10^4	3133	+0.8	-0.1	-0.3	each ± 0.1

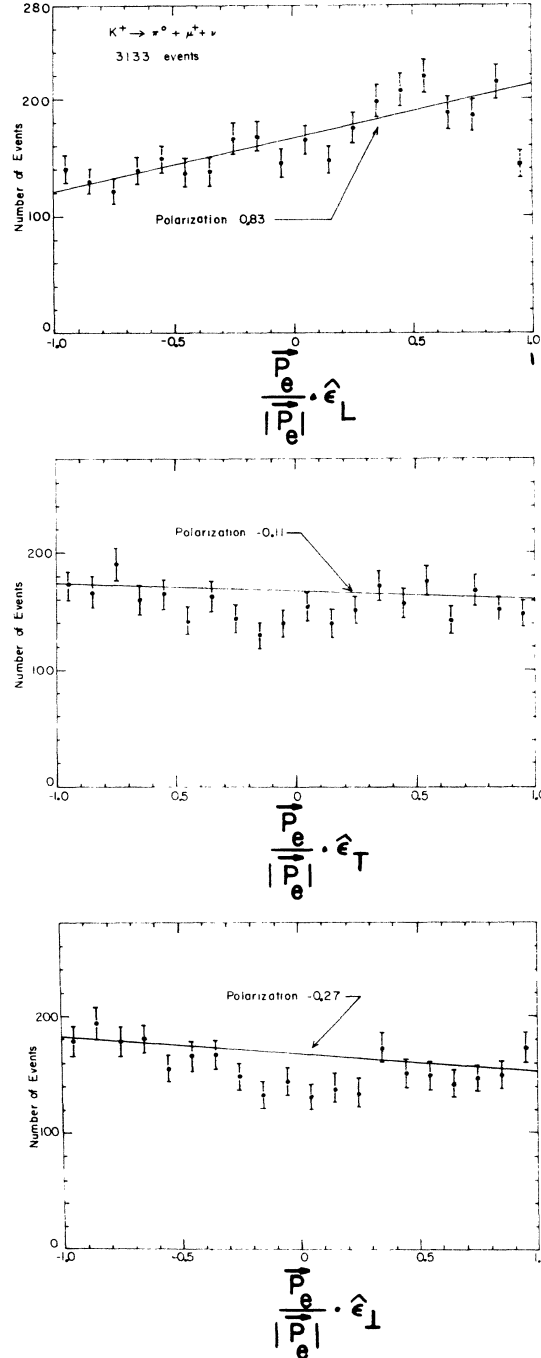


FIG. 6. Angular distribution of the electron momentum vector in μ - e decays, from 3133 $K_{\mu 3}^+$ events, referred to the axes $\hat{\epsilon}_L, \hat{\epsilon}_T, \hat{\epsilon}_1$. The lines drawn are normalized to the 3133 events with $p_e \cdot \hat{\epsilon}_L < 0.9$. The dip in the lower two graphs for cosines near zero reflects the loss of events with $p_e \cdot \hat{\epsilon}_L > 0.9$. Because of this cut, the data points are not expected to fit the solid lines.

average value of q^2 , the square of the momentum transfer to the leptons, in the K^+ rest frame

$$q^2 = m_K^2 + m_{\pi^0}^2 - 2m_K E_{\pi^0}.$$

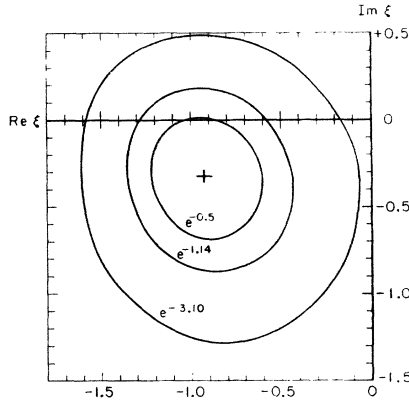


FIG. 7. Likelihood functions for ξ assumed complex and constant, from 3133 $K_{\mu 3}^+$ Events. The $e^{-1.14}$ contour corresponds to the limit of 1 standard deviation about the most probably value, $\text{Re}\xi = -0.9$, $\text{Im}\xi = -0.3$.

Most of our data are in the low- q^2 (high- π^0 -energy) region of the Dalitz plot. The bins were chosen to give equal accuracy in the measurement of ξ ; they are of unequal size, due to the varying sensitivity of the polarization method over the Dalitz plot. As noted in Table IV, for high- q^2 (low- T_{π^0}) events, we found the μ^+ strongly polarized along the perpendicular axis. For progressively lower bins in q^2 , this perpendicular component decreases, and the μ^+ becomes almost fully longitudinally polarized. This general variation of the polarization components over the Dalitz plot compares favorably with that predicted by Eq. (3) and illustrated in Fig. 1.

We analyzed our data by the maximum-likelihood method previously described to determine the value of the parameter ξ . As discussed in the Introduction, ξ may be complex as well as energy-dependent. Figure 7 shows the result of the likelihood analysis of all the $K_{\mu 3}$ events for ξ assumed complex, but constant. The three contours enclose 40, 67, and 96% of the volume under the two-dimensional likelihood function; the solution given in Table V uses the middle contour as the limit of 1 standard deviation. We list additionally, in Table V, the results for complex ξ from data binned in q^2 . For each bin ξ is assumed constant; the errors again correspond to the middle ($e^{-1.14}$) contour. Time-reversal invariance requires ξ be real; our measurement from all the data is consistent with $\text{Im}\xi=0$, as can be seen in

TABLE V. Results for complex ξ .

$\langle q_{av}^2 \rangle$ (MeV ²)	Events	Re ξ	Im ξ
3.70×10^4	2258	$-1.0_{-0.9}^{+1.0}$	-0.8 ± 0.9
7.18×10^4	488	$-2.0_{-0.8}^{+0.9}$	$-0.7_{-1.0}^{+0.9}$
9.09×10^4	265	$-0.7_{-0.9}^{+1.2}$	$-0.3_{-1.0}^{+0.9}$
11.0×10^4	122	$-0.4_{-1.4}^{+2.2}$	$+0.8_{-1.2}^{+1.8}$
all events	3133	$-0.9_{-0.4}^{+0.5}$	-0.3 ± 0.5

TABLE VI. Results for ξ assumed real.

$\langle q_{av}^2 \rangle$ (MeV ²)	Events	Re ξ (Im $\xi=0$)	P_{total}
3.70×10^4	2258	-0.9 ± 0.6	0.9 ± 0.1
7.18×10^4	488	-1.9 ± 0.55	0.8 ± 0.2
9.09×10^4	265	$-0.7_{-0.6}^{+0.7}$	1.1 ± 0.3
11.0×10^4	122	$-0.2_{-0.7}^{+0.6}$	1.2 ± 0.4
all events	3133	-0.95 ± 0.3	0.9 ± 0.1

Fig. 7. This conclusion is unchanged by measuring $\text{Im}\xi$ in separate bins in q^2 . In terms of a phase angle ϕ defined by

$$\xi = |\xi| e^{i\phi},$$

we find

$$|\xi| = 1.0 \pm 0.5, \quad \phi = (200 \pm 30)^\circ,$$

with the error assigned from the $e^{-1.14}$ contour. This result is consistent with the requirement of time-reversal invariance that ϕ be 0° or 180° .

Assuming ξ to be real and constant, we obtain the results given in Table VI. The errors quoted are those appropriate to a one-dimensional likelihood. The values for $\text{Re}\xi$ from different bins in q^2 are consistent with each other, and with the result for all the data

$$\text{Re}\xi = -0.95 \pm 0.3 \quad (\text{Im}\xi=0).$$

In Fig. 8, we have plotted our measurements of $\text{Re}\xi$ as a function of q^2 ; they do not show any significant dependence of $\text{Re}\xi$ upon q^2 . Table V shows that this conclusion is valid for complex ξ as well. To make this conclusion more quantitative, we express the energy dependence of ξ as

$$\xi(q^2) = \xi_0 (1 + \lambda q^2 / m_{\pi^0}^2).$$

We can analyze the data in a two-parameter likelihood to obtain the constants ξ_0 and λ , assuming ξ real. Our result is

$$\xi_0 = -1.2, \quad \lambda = -0.04,$$

with the contours giving the limits of 1 and 2 standard deviations as shown in Fig. 9. For any value of λ less than 0.3 in magnitude, ξ must be negative to be compatible with the data. An analysis of our data for q^2 dependence of the form

$$\xi(q^2) = \xi_0 m^2 / (m^2 + q^2)$$

gives the result that any values of m greater than

TABLE VII. Results of measurements of K^+ mean life.

Decay mode	Events	Mean life	
		(channels)	(nsec)
$K_{\mu 3}$	1635	6.0 ± 0.5	13.2 ± 1.6
$K_{\mu 2}$	773	6.6 ± 0.7	14.5 ± 2.0
$K_{\pi 2}$	278	6.3 ± 1.2	13.9 ± 2.9
combined result		6.2 ± 0.4	13.5 ± 1.5

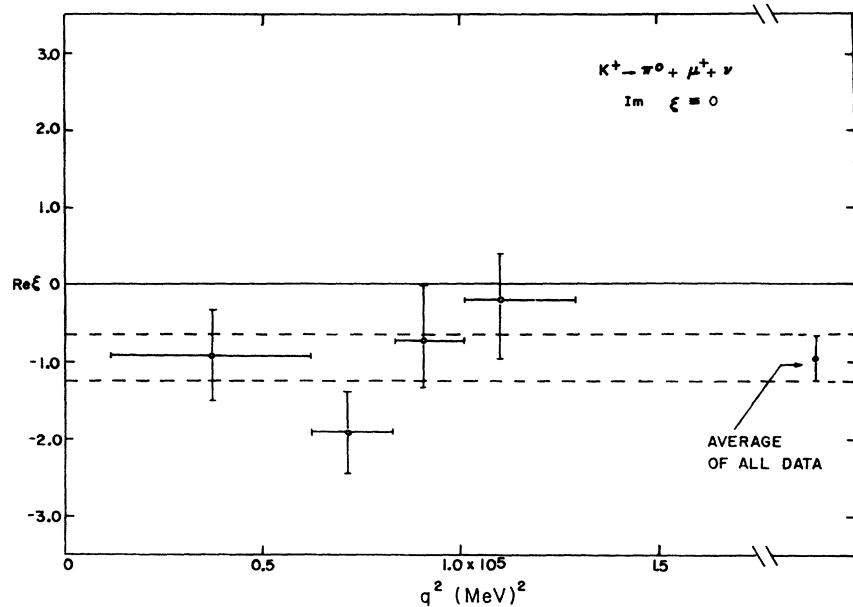


FIG. 8. Results of likelihood analyses for ξ assumed real and constant, from data in four bins of q^2 . The result for all the data is also shown: $\xi = -0.95 \pm 0.3$.

500 MeV are equally good; the corresponding values of ξ_0 are all ~ -1.0 . We find the lower limit for acceptable m to be ~ 250 MeV.

Given the values of ξ listed in Table VI, we analyzed the data to determine the magnitude of the μ^+ polarization, P_{total} , along the direction predicted for each event. For all the data, we found this component to be $+0.9 \pm 0.1$, in agreement with the expected value of $+1.0$. The results for P_{total} from data in separate bins of q^2 are listed in Table VI; they are consistent with each other, and with the predicted value. We obtain

essentially the same values if, instead of assuming ξ to be real, we calculate P_{total} using the results for complex ξ given in Table V.

B. Measurement of K^+ Mean Life

We determined the K^+ mean life for each of the decay modes $K_{\mu 3}$, $K_{\mu 2}$, and $K_{\pi 2}$. For each event, the observed time between the K^+ stop and the subsequent decay signal was digitized and recorded on film with the spark-chamber tracks. Table VII gives our results for

TABLE VIII. Recent measurements of ξ in K^+ and K^0 decay.

Decay	Experiment	Results for ξ assumed constant	
		$\text{Im}\xi=0$	$\text{Im}\xi \neq 0$
Carpenter <i>et al.</i> ^a	$K_{\mu 3}^0$	Decay spectrum	$\xi = 1.2 \pm 0.8$
Auerbach <i>et al.</i> ^b	$K_{\mu 3}^0$	μ^+ perpendicular polarization	$\xi = -1.2 \pm 0.5$
Young <i>et al.</i> ^c	$K_{\mu 3}^0$	μ^+ transverse polarization	for $\text{Re}\xi = -1.3$, $\text{Im}\xi = -0.01 \pm 0.07$
Garland <i>et al.</i> ^d	$K_{\mu 3}^+$	Branching ratio $K_{\mu 3}^+/K_{e 3}^+$	$\xi = +1.0 \pm 0.5^e$
Eisler <i>et al.</i> ^f	$K_{\mu 3}^+$	Decay spectrum	$\xi = -0.5 \pm 0.9$
Abrams <i>et al.</i> ^g	$K_{\mu 3}^0$	μ^+ total polarization	$\xi = -1.6 \pm 0.5$
Helland <i>et al.</i> ⁱ	$K_{\mu 3}^0$	μ^+ total polarization	$\xi = -1.75_{-0.2}^{+0.5}$
Botterill <i>et al.</i> ^j	$K_{\mu 3}^+$	Branching ratio $K_{\mu 3}^+/K_{e 3}^+$	$\xi = -0.08 \pm 0.15$
Bettels <i>et al.</i> ^k	$K_{\mu 3}^+$	μ^+ total polarization	$\xi = -1.0 \pm 0.3$
Eichten <i>et al.</i> ^l	$K_{\mu 3}^+$	Branching ratio $K_{\mu 3}^+/K_{e 3}^+$	$\xi = -0.6 \pm 0.2$
This experiment ^m	$K_{\mu 3}^+$	μ^+ total polarization	$\xi = -0.95 \pm 0.3$
			$\text{Re}\xi = -0.9_{-0.4}^{+0.5}$ $\text{Im}\xi = -0.3 \pm 0.5$

^a D. W. Carpenter *et al.*, Phys. Rev. **142**, 871 (1966).
^b L. B. Auerbach *et al.*, Phys. Rev. Letters **17**, 980 (1966).
^c K. K. Young *et al.*, Phys. Rev. Letters **18**, 806 (1967).
^d R. Garland *et al.*, Phys. Rev. **167**, 1225 (1968).
^e The quoted errors in the branching-ratio measurement and in the result for ξ are inconsistent. We have adjusted the error in ξ to correct for this discrepancy.
^f F. R. Eisler *et al.*, Phys. Rev. **169**, 1090 (1968).
^g R. J. Abrams *et al.*, Phys. Rev. **176**, 1603 (1968).

^h We have adjusted the errors to make the quoted results comparable with results of other experiments.
ⁱ J. A. Helland *et al.*, Phys. Rev. Letters **21**, 257 (1968).
^j D. R. Botterill *et al.*, Phys. Rev. Letters **21**, 766 (1968).
^k J. Bettels *et al.*, Nuovo Cimento **56A**, 1106 (1968).
^l T. Eichten *et al.*, Phys. Letters **27B**, 586 (1968).
^m A brief account of this experiment is given in D. Cutts *et al.*, Phys. Rev. Letters **20**, 955 (1968).

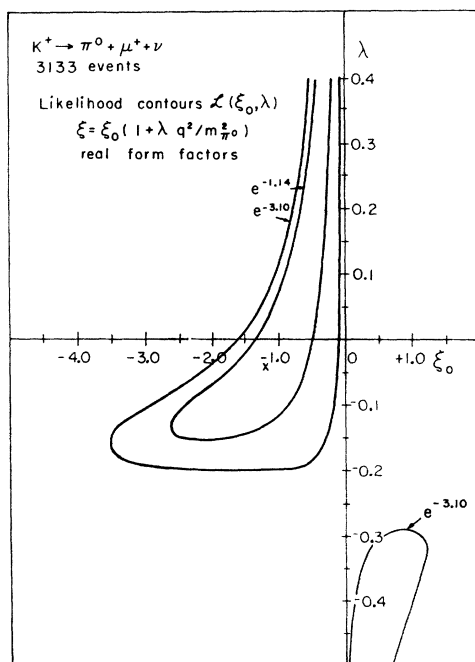


FIG. 9. Likelihood function for ξ real and energy-dependent, from 3133 $K_{\mu 3}$ events. The $e^{-1.14}$ and $e^{-3.10}$ contours give the limits of 1 and 2 standard deviations.

$K_{\mu 3}$, $K_{\mu 2}$, and $K_{\pi 2}$ lifetimes. Each of these measurements is consistent with each other, as expected for observed lifetimes of different decay modes of the same particle. If we combine the three measurements of the K^+ mean life, we have $\tau = 13.5 \pm 1.5$ nsec, in reasonable agreement⁹ with the accepted value, $\tau = 12.34 \pm 0.05$ nsec.

VII. DISCUSSION

In a study of the muon polarization direction for completely reconstructed $K_{\mu 3}^+$ decays, we measure the form factor $\xi(q^2)$. Assuming ξ to be real and independent of q^2 , we find

$$\xi = -0.95 \pm 0.3.$$

Since the direction of the μ^+ polarization vector is predicted as a function of $\xi(q^2)$ for each event of specified kinematics, the experiment allows a determination

of the q^2 dependence. Our measurement of the muon polarization is directly sensitive also to the presence of an imaginary part of ξ , corresponding to the violation of time-reversal invariance, as we determine the polarization component out of the decay plane. The results indicate that the form factor $\xi(q^2)$ is real and constant, within the limits given in Sec. VI.

We find the magnitude of the μ^+ polarization along the direction predicted by our result for ξ to be 0.9 ± 0.1 . This value confirms the prediction of the two-component neutrino theory that the muon be fully polarized along some direction. Background events in the $K_{\mu 3}$ data or systematic errors in the reconstruction of events reduce the apparent magnitude of the muon polarization; our measurement suggests that these effects are small.

Previous measurements of $\xi(q^2)$ in K^+ and K^0 decay are summarized in the review article of Lee and Wu.¹⁰ Recently published experiments to determine ξ which are not included in this review are listed in Table VIII. The results for ξ from K^0 experiments are consistent with the results of this experiment, in agreement with the requirement of the $\Delta I = \frac{1}{2}$ rule that ξ be the same in K^+ and K^0 decay. Experiments which determine ξ from a muon polarization measurement are in good agreement with each other, but in general disagreement with early results for ξ from measurements of the relative $K_{\mu 3}/K_{e 3}$ branching ratio. The determination of ξ from branching-ratio measurements requires the assumption of μ - e universality—specifically, the assumption that the form factors in $K_{e 3}$ and $K_{\mu 3}$ decay are identical. The branching-ratio technique has the experimental complication that detection efficiencies must be accurately known, a requirement absent from total-polarization measurements. As seen in Table VIII, the most recent branching-ratio experiment gives a result for ξ compatible with the results from polarization measurements, and in agreement with μ - e universality.

ACKNOWLEDGMENTS

We are grateful to Professor Emilio Segrè for his encouragement of this work and for many helpful discussions. Dr. Peter Kijewski and Dr. Min Chen contributed heavily to both the data taking and the analysis. We wish to thank W. Hartsough for his efficient operation of the Bevatron.

⁹ Data compilation of A. H. Rosenfeld *et al.*, Rev. Mod. Phys. 40, 77 (1968).

¹⁰ T. D. Lee and C. S. Wu, Ann. Rev. Nucl. Sci. 16, 471 (1966).